ACS APPLIED MATERIALS & INTERFACES

Research Article

www.acsami.org

Method to Form a Fiber/Growth Factor Dual-Gradient along Electrospun Silk for Nerve Regeneration.

Tony M. Dinis,*[,†,‡] Roberto Elia,[‡] Guillaume Vidal,[†] Adrien Auffret,[†] David L. Kaplan,[‡] and Christophe Egles[†,§]

[†]CNRS UMR 7338: BioMécanique et BioIngénierie Centre de recherche, Université de Technologie de Compiègne, BP 20529 Rue Personne de Roberval, 60205 Compiègne, France

[‡]Department of Biomedical Engineering, Tufts University, 4 Colby Street, Medford, Massachusetts 02155, United States

[§]Department of Oral and Maxillofacial Pathology, School of Dental Medicine, Tufts University, 55 Kneeland Street, Boston, Massachusetts 02111, United States

ABSTRACT: Concentration gradients of guidance molecules influence cell behavior and growth in biological tissues and are therefore of interest for the design of biomedical scaffolds for regenerative medicine. We developed an electrospining method to generate a dual-gradient of bioactive molecules and fiber density along electrospun nanofibers without any post spinning treatment. Functionalization with fluorescent molecules demonstrated the efficiency of the method to generate a discontinuous concentration gradient along the aligned fibers. As a proof of concept for tissue engineering, the silk nanofibers were functionalized with increasing concentrations of nerve growth factor (NGF) and the biological activity was assessed and quantified with rat dorsal root ganglion (DRG) neurons cultures. Protein assays showed the absence of passive release of NGF from the functionalized fibers. The results demonstrated that the NGF concentration gradient led to an oriented and increased growth of DRG neurons (417.6 ± 55.7 μm) compared to a single uniform NGF concentration (264.5 ± 37.6 μm). The easy-to-use electrospinning technique combined with the multiple molecules that can be used for fiber functionalization makes this technique versatile for a broad range of applications from biosensors to regenerative medicine.

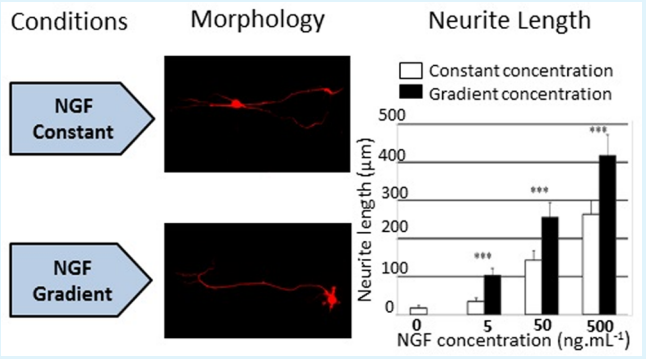

KEYWORDS: *nerve growth factor, concentration gradient, tissue engineering, electrospinning, silk, regenerative medicine*

1. INTRODUCTION

Severe peripheral nerve damage affects 200 000 patients in the United States and 300 000 in Europe each year.[1] Unlike in the Central Nervous System, axonal regeneration and recovery is possible after peripheral nerve injury.[2] Spontaneous nerve regeneration can occur for short nerve gaps, while repairing large nerve gaps (>10 mm) remains a major challenge for surgeons.[3] Indeed, peripheral nerve regeneration is based on a highly organized and complex biological system composed of multiple cells, growth factors and extracellular matrix molecules (ECM). To date, the most effective way to repair large gaps remains autologous nerve grafting. Even if this technique is considered the clinical standard for peripheral nerve gap repair, there are many limitations due mainly to limited donor site availability, morbidity and surgical complications due to the need for two or more operative procedures.[4] For very short gaps (<5 mm), biological tissues such as arteries, veins or muscle can also be used, however these allografts have shown varying success.[5] In recent years, advances have been made in the development of new biomaterials as nerve guidance conduits composed of synthetic, natural or composite polymers systems.[6−8] These nerve guidance conduits should facilitate directional axonal growth from the regenerating nerve, protect the regenerating nerve from fibrous tissue barriers and allow diffusion of growth factors and nutrient exchange. Despite the fact that the FDA has approved some nerve guidance systems; the clinical reality is that these biomaterials have been far from effective for nerve repair after injury or trauma.[9]

Scaffolds prepared via electrospinning allow aligned fibrous matrix formation with good porosity and mechanical properties using native and/or synthetic polymers with nanoscale structures similar to native extracellular matrices. Recently, silk electrospun fibers have been applied in the investigation of tissue engineering for biomedical applications.[10,11] Silk fibroin is a natural protein, well-known for its robust mechanical properties and excellent biocompatibility.[12] The degradation rate of silk biomaterials can be tailored from months to years

Received: June 26, 2014
Accepted: September 9, 2014
Published: September 9, 2014

after implantation in vivo, based on processing procedures employed during materials formation.[13]

Moreover, electrospun silk fibers can also be postmodified via chemical treatments yielding improved cell proliferation, cell adherence, and growth.[14] Bioactive molecules, such as adhesion or growth factors added to the spinning solution remain active and available in the electrospun fibers.[15] Many different types of bioactive molecules have been incorporated into silk scaffolds of electrospun nanofibers, including growth factors, biomimetic peptides and metals.[16−18] Growth factors are endogenous proteins capable of binding to cell receptors and directing cellular activities.[19] Nerve growth factor (NGF) is a neurotrophic factor known for promoting the survival and differentiation of developing neurons (sensory and sympathetic neurons) in the peripheral nervous system. NGF delivery enhanced neuronal outgrowth and also can be used as a chemoattractant axon guidance cue.[20,21]

Gradients of chemicals and/or biological molecules on the surface of scaffolds influence cell alignment of fibroblasts, neurons, and bone marrow stem cells.[22−25] The guidance of growth cones, which are the functional unit for axonal growth, can be mediated by several growth factors. In fact through the growth cones, axons sense guidance cues offered by the concentration gradient, allowing for regeneration.[26] This signaling is dependent on gradients of concentration.[27] Some studies have observed the behavior of extending or regenerating axons in response to gradients of growth factors within hydrogels and microfluidic chambers.[28,29] Hydrogels are one of the most utilized scaffolds for tissue repair; however they do not preserve the alignment of the axonal growth cones. Conversely, although microfluidic systems preserve alignment, the pressure differences created by the devices cause a biological stress, which can reduce cell survival.[29]

In the present study, we describe the development of a functional NGF gradient on aligned silk fibers and characterize the electrospun mat using physicochemical techniques as well as neuronal cultures. To our knowledge, this work is the first study to demonstrate the production of an aligned electrospun functionalized scaffold that exhibits coordinated NGF and fiber density gradients along the longitudinal axis of the fibers, without any postspinning chemical modification. To stimulate unidirectional axonal outgrowth is the main challenge for peripheral nerve regenerative reconstruction. The effects of this new nanofibrous gradient on the orientation and rate of neuron growth were examined on primary sensory neurons from rats DRGs. The production of this "dual gradient" (growth factor and fibers) into aligned silk nanofibers focused the axonal guidance cue in only one direction and stimulated axonal outgrowth.

2. MATERIALS AND METHODS

2.1. Materials. Silkworm cocoons from *Bombyx mori* were purchased from Tajima Shoji Co. (Yojohama, Japan). All Chemicals products were purchased from Sigma-Aldrich, Inc. (St. Louis, MO, USA). Slide-a-Lyzer dialysis cassettes were purchased from Pierce, Inc. (Rockford, IL, USA). All media cell products were purchased from Gibco, life technologies SAS (France). NGF was purchased from R&D Systems, Inc. (Minneapolis, MN, USA)

2.2. Silk Fibroin Solution Preparation. Silk fibroin was extracted from *B. mori* silkworm cocoons and solutions were prepared following previously published procedures.[30] Briefly, cocoons were cut into small pieces (∼5 g) and immersed into boiling for 30 min in 2 L of an aqueous solution of 0.02 M Na_2CO_3. The degummed fibers were rinsed for 20 min, three times with cold deionized (DI) water, then allowed to dry for 48 h at room temperature. Dried silk fibroin fibers were solubilized in 9.3 M LiBr solution (1 g of dried fibers:4 mL of LiBr solution) at 60 °C for 4 h. Silk solutions were dialyzed against DI water using Slide-a-Lyzer dialysis cassettes (membrane MWCO 3500) for 72 h to remove salts. Silk fibroin solution was centrifuged twice to remove insoluble particulates. The final concentration of aqueous silk fibroin solution was 6−7 wt %, which was calculated by weighing the remaining solid after drying. Solution was then concentrated by dialyzing against 15% (w/v) PEG (6000 g/mol) for 4 h to produce ∼10 wt % silk fibroin. Silk solutions were stored at 4 °C.

2.3. Preparation of Spinning Fluorescent or Functionalized Solution. Silk fibroin concentrated at 10 wt % solutions were mixed with 5 wt % poly(ethylene oxide) (PEO, M_w = 900 000) in a 4:1 (v/v) silk/PEO ratio to produce an 8 wt % silk fibroin solution in order to improve the solution viscosity before spinning.[31] To generate fluorescently labeled electrospun fibers, Rhodamine-B (Merck Chemicals, Germany) (0.1 g) was added to the silk solution to produce a 100% solution and diluted to 10% and 1%.The three different concentration solutions of silk/rhodamine-B at 100, 10, and 1% were electrospun successively to demonstrate the presence of the gradient. 70 kDa fluorescein isothiocyanate-dextran (Sigma-Aldrich, Inc. St. Louis, MO, USA) at 10% was added into the silk solution prior spinning. To functionalize the spinning solution, NGF reconstituted in PBS containing 0.1% bovine serum albumin solution, was added to the silk solution at 500, 50, and 5 ng/mL.

2.4. Aligned Silk Electrospun Scaffolds. Spinning solution was delivered through a 16G stainless-steel capillary, at a flow rate of 5 μL min^{-1} using a Sage syringe pump (Thermo Scientific, Waltham, MA). The capillary was maintained at a voltage of 12 kV using a high voltage power supply (Gamma High Voltage Research ES-30P, Ormond Beach, FL, USA) and was mounted at the center of a 10 cm-diameter aluminum plate. To fabricate axial fiber alignment, two electrically independent, 8 cm width × 0.3 cm thick, flat, zinc-plated steel plates served as collectors. The plates were mounted on 25 cm high ceramic stands fastened to adjustable PVC legs that allowed angle and spacing adjustments. The plates were positioned 16 cm below the droplet and 10 cm from each other in different trials covered by electrical tape (3M, St. Paul, MN) in order to support glass coverslips. Electrospun silk-fibroin fibers were collected on the glass coverslips for 3 min total deposition time. Fiber alignment was controlled by connecting each collector to a separate electrically independent output of a switch. During electrospinning, first one collector was provided with electrical ground for a half period, normally 1.5 s, whereas the second collector was disconnected. Then for the next half period, the ground was switched to the second collector while the first collector was disconnected. After a full period, it was switched back to the first collector. This oscillation of ground was maintained continuously until the electrospinning process was completed. Fibers deposited between the collectors. The cover-glasses coated with silk fibers were then stored in dry atmosphere until needed.

2.5. Scaffold Characterization. To demonstrate the discontinuous gradient, fluorochrome fibers along the *y*-axis without chemical modification post spinning fibers were imaged on a Zeiss Axiovert 40 CFL (Thornwood, NY) microscope equipped with three filter (470/500, 350/460, 560/630 Exc/Emi) and QCapture (Surrey, BC) image capture software. Pixel intensity of the fluorescence images was measured with "Scion Imaging" software (NIH). Electrospun NGF-silk gradients on glass coverslips were sputter-coated with gold/palladium and then evaluated using a field-emission Scanning Electron Microscope (SEM, Supra 55, Zeiss, NY) at 5 kV. To determine fiber diameters and alignment all SEM images were analyzed by ImageJ and Matlab software packages.

Fourier Transform infrared spectroscopy (FTIR) analysis of the gradient electrospun mats was performed with a Jasco FT/IR-6200 spectrometer (Easton, MD), equipped with a multiple reflection, horizontal Miracle attenuated total reflectance (ATR) attachment (ZnSe crystal, from Pike Tech., Madison, WI). Each measurement incorporated 64 scans with nominal resolution of 4 cm^{-1} (wavenumber from 600 to 4000 cm^{-1}) that were Fourier transformed using a Genzel-Happapodization. To identify secondary structures in the

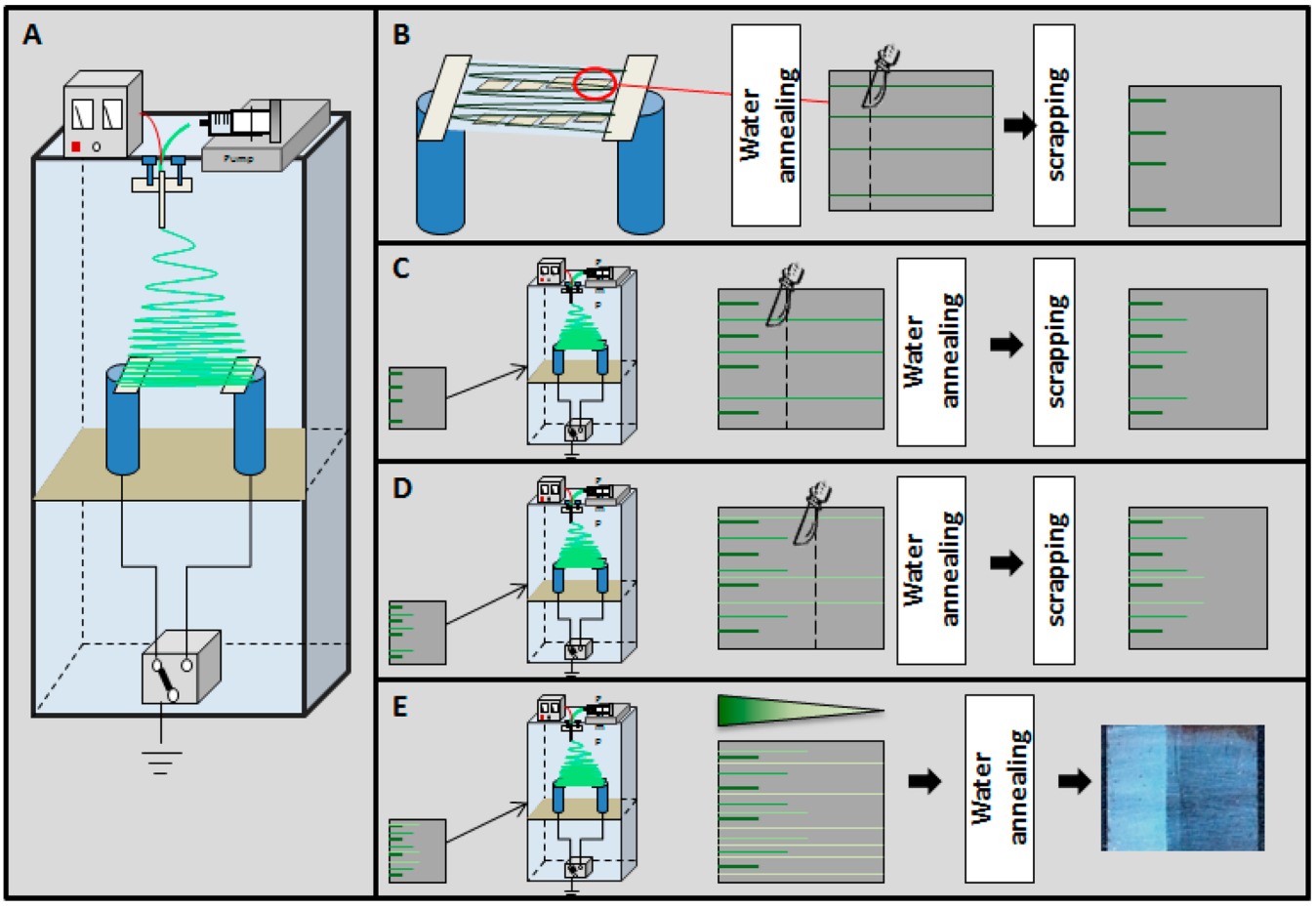

Figure 1. Schematic of NGF-silk gradient aligned nanofibers via electrospun fabrication. (A) Silk aligned nanofibers were collected via to an oscillating ground deposition system, consisting of two zinc-coated steel plates bridged with nonconductive electrical tape which hold the glass coverslips support. Four spinning solutions with NGF at different concentrations were used to form the aligned electrospun fibers with NGF gradients. (B) High concentration of NGF-Silk solution was spun on the glass coverslips for 3 min and all but 4 mm of fibers were cut away. (C) Glass coverslips from B were spun with medium concentration of NGF-Silk solution, and all but 7 mm of fibers were left on the glass slide. (D) Glass coverslips from C were spun with the lower concentration of NGF-Silk solution, and all but 10 mm of the fibers were left on the slides. (E) Silk solution was spun for 10 min on the top of D coverslips. After each deposition the fibers were annealed for 30 min, with the final deposition receiving overnight annealing, all to induce β sheet crystallization of the silk to prevent aqueous solubility.

protein samples from the absorption spectra, peak positions of the amide I region (1595−1705 cm^{-1}) absorption from Fourier self-deconvolution were analyzed. Curve fitting was performed using Jasco Spectra-Manager Analysis Software (Jasco, Easton MD), as previously described.[10,31,32]

2.6. In Vitro NGF Release and Bioavailability. NGF gradient electrospun nanofibers on glass coverslips (n=3) were incubated in 2 mL of PBS containing 0.1% BSA with 0,02% Tween20 at 37 °C and 150 μL of the solution was collected after 1, 6, 24, 72, and 168 h and stored at −80 °C. To estimate recovery percentage of NGF on fibers, coverslips gradient fibers were dissolved in 10 μL of 9.3 M LiBr for 30 min at room temperature and dialyzed again 1 L of deionized (DI) water for 6 h. NGF concentration was quantified with the ChemiKine Growth Factor Sandwich ELISA Kit (Millipore, France) according to the manufacturer's instructions.

2.7. Cell Cultures. DRG cells were isolated from male Sprague−Dawley rats (1−2 months old) using a modified protocol adapted from a previously published procedure[33] for rats. All procedures were performed in accordance with the European Directive 2010/63/EU. DRGS were extracted from rat spinal cord and incubated in 2.5% collagenase (Sigma) for 15 min at 37 °C. Then, DRGs were centrifuged at 500g for 1 min, the supernatant was removed and the pellet was resuspended and incubated in trypsin (Sigma) 0.5% and DNase I (Sigma) at 1 mg/mL^{-1} for 15 min at 37 °C. After another centrifugation, 500g for 1 min, the DRGs were washed with F-12 medium and dissociated with a fire-polished Pasteur pipet. The mean yield of cells obtained per rat was 100,000 with 90% viability. Glass slides were coated with poly lysine/laminin before seeding, as described in Malin et al.[33] Moreover glass slides were treated in water 24 h before culture in order to extract PEO from electrospun silk fibroin fibers mat.[34] Culture medium consisted of 37 °C prewarmed F-12 medium, 10% horse serum, and 100 U/mL^{-1} and was changed every 3 days.

2.8. Immunostaining. Cells were fixed after 72h postseeding in a polyoxymethylene (paraformaldehyde) solution at 4% in PBS for 15 min, at room temperature and rinsed three times with PBS. Membrane permeabilization was performed with 0.5% Triton X-100 in PBS for 5 min at room temperature and rinsed twice with PBS. Samples were incubated overnight at 4 °C in 1% bovine serum albumin (BSA) in PBS solution to minimize nonspecific staining. Primary antibodies against βIII tubulin (Sigma-Aldrich, France) were diluted (1:150) in PBS/BSA 0.1% (w/v) and incubated at room temperature in the dark for 1 h. Samples were washed twice with 0.1% BSA in PBS. Cy3-conjugated secondary antibody (cy3 goat antirabbit IgG, Jackson Immunoresearch), 40,6-diamidino-2-phenylindole (DAPI; 1 μg.mL-1, Sigma) and Phalloidin-X5- 505 (0.16 nmol ml-1, Fluoroprobes, France) were added and incubated at room temperature in the dark for 1 h. The samples were then rinsed three times with PBS, mounted in Mowiol and observed using a LEICA DMI 6000 microscope.

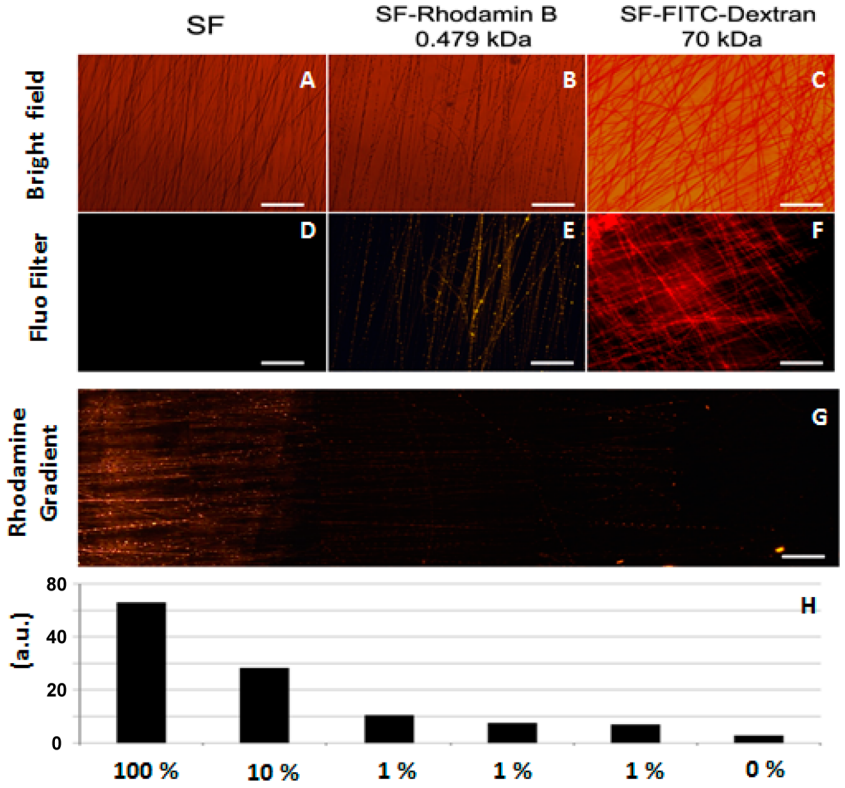

Figure 2. Fluorescence imaging to show the efficiency of the gradient. (A) Unmodified silk fibroin, (B) silk-rhodamine-B, or (C) silk-FITC-dextran functionalized fibroin were observed by fluorescent microscopy in bright field and via (D−F) fluorescent filter, respectively. Rhodamine fluorescence of aligned fibers (G) on a 22 mm glass slide coupling different rhodamine concentrations (100, 10, 1, and 0%). (H) Fluorescence intensities measured along the rhodamine gradient from the aligned slide fibers in G. Scale bars: 20 μm.

2.9. Morphometric Analysis. Images were analyzed using ImageJ software. Low signal was filtered out using a threshold based on intensity (the silk fibers and background noise present lower pixel intensities than the cell bodies and neurites). In each image, the number of cells was determined using the signal from DAPI staining. Then each neurite was isolated using the tubulin staining and its length was measured using a macro created on ImageJ. Multiple points were drawn along the length of the primary and longest axon, in order to follow the curves and determine the length. The coordinates were then used to calculate distances between two points. In a final step, all distances were added to obtain the axon length. More than 100 axons were measured per concentration.

2.10. Statistical Analysis. Statistical analysis was performed using InStat software. Values were expressed as mean ± standard deviation (mean ± SD). Neurit length and neurite per cell were compared using one way analysis of variance (ANOVA). A p-value less than 0.05 was considered to be significant.

3. RESULTS

3.1. Fabrication of Gradient Nanofibrous Scaffolds. Silk fibroin solution at 8 wt % was prepared for spinning. Protein was added to the spinning solution to get one stock standard solution taken to be 100%. Stock solution was diluted to obtain solutions at 10% and 1%. Electrical tape was connected between two pieces of conductive substrates, which allowed the alignment of fibers using oscillation of the ground (Figure 1A). The stock standard solution (100%) was first electrospun onto glass coverslips. After spinning, samples were annealed and electrospun fibers were located on the first 4 mm on one side of the coverslip were retained, while, the rest of the fibers were cut and discarded (Figure 1B). The same process was repeated twice more on the same glass cover with diluted concentrations of protein solution at 10 and 1% successively. Seven millimeters from the top side of the coverslip were kept for the 10% solution and then 10 mm of fibers for the 1% concentration solution. Finally, the glass slides were electrospun with silk solution to cover the 22 mm of the coverslips with silk nanofibers (Figure 1C−E).

Using this method, a discontinuous gradient of two parameters (i) protein concentration and (ii) density of silk fibers was produced along the aligned nanofibers. One side of the slides presents highly functionalized fibers whereas the opposite side only consisted of silk nanofibers without a functional component. By producing nanofibers by four successive electrospinning processes, the density of silk aligned nanofibers increased along the slide. At the end of the process, slides presented a "dual-gradient" characterized by increasing concentrations of protein and the density of aligned silk nanofibers.

3.2. Gradient Assessment by Fluorescence. Fluorochromes, rhodamine (479 Da) and dextran FITC (70 kDa) were added to the silk solution before spinning. Electrospun fibers were first observed in bright field (Figure 2A−C) and then under fluorescence. As expected, no fluorescence was detected in the absence of the fluorochrome (Figure 2D), whereas a fluorescence signal was observed on the surface of fibers after spinning fluorochrome solutions (Figure 2E, F). Using molecules with a higher molecular weight such as dextran FITC, fluorescence intensity was detected in the mat, demonstrating that molecules with an average molecular weight can also be incorporated inside the silk fibers. A gradient consisting of aligned fibers functionalized with rhodamine along the y-axis were observed using this approach (Figure 2G).

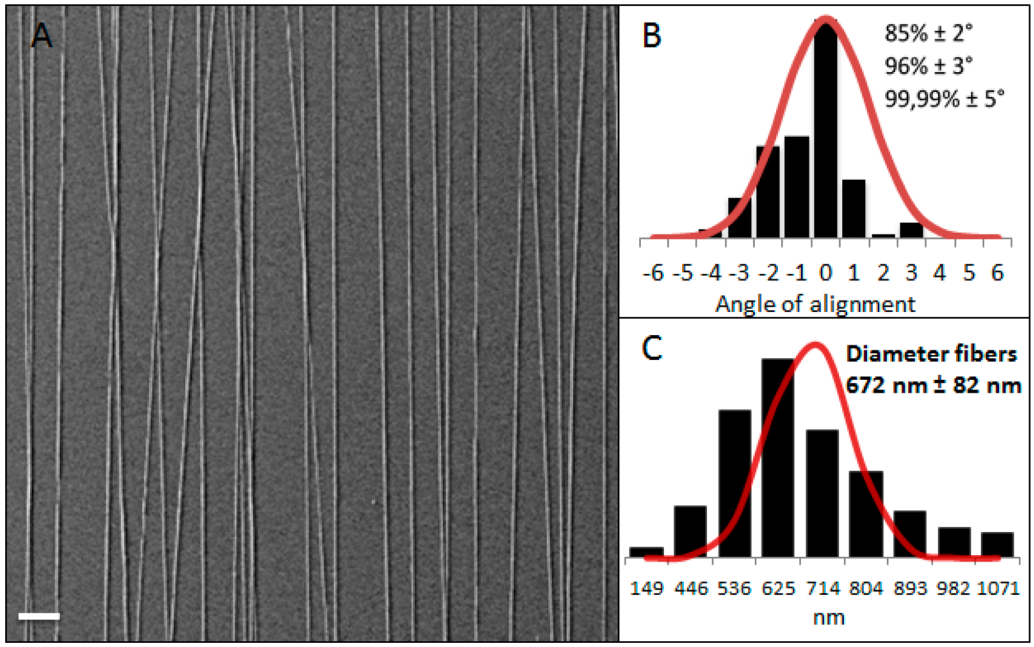

Figure 3. Characterization of the gradient of aligned electrospun fibers. (A) SEM image of aligned gradient NGF-silk nanofibers on glass slides; (B) Distribution of fiber alignment from glass slides, with 85% of fibers present at an angle of deviation less than 2°. (C) Distribution of fiber diameter from glass slides. Bars represent measured data, and the associated curves are the best fit Gaussian form. Alignment and mean diameter of electrospun fibers were determined as described in the Material and Methods. Scale bars: 5 μm.

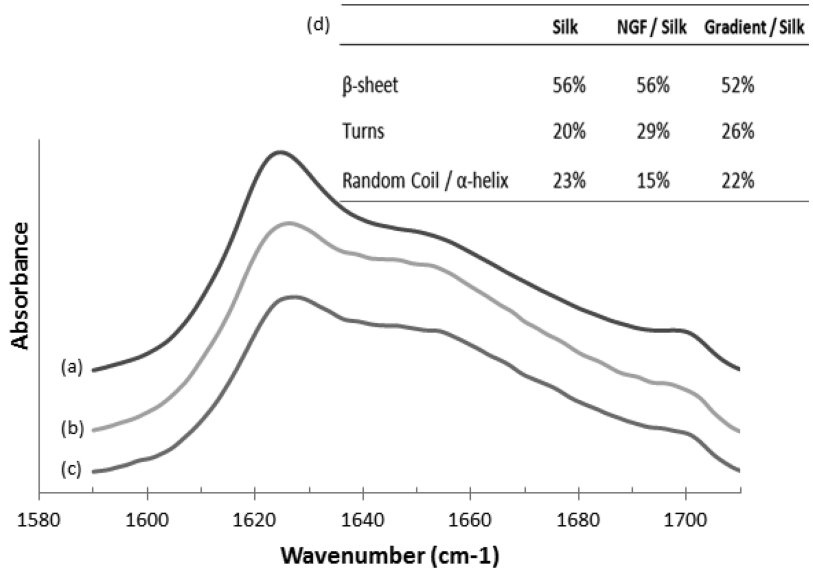

Figure 4. FTIR spectra of electrospun materials prepared by water annealing. FTIR spectra of (a) silk fibroin electrospun mats; (b) silk fibroin functionalized with NGF and (c) NGF-silk gradient electrospun mats. (d) Table of the secondary structure of the silk fibroin. All samples were treated by water-annealing overnight.

Fluorescence intensities were analyzed on the slide part which fibers retained consist on the standard solution (100%), and then fibers from diluted solutions (10%, 1%) and 0%. Four different intensity values characterized the different steepness of the gradient formed. The results were 53.1 for the higher, 28.4 for medium, and 10.5 for low concentration. As a control, when no rhodamine was added, only a weak autofluorescence of the fibers was detected with a value of 2.84.

3.3. Characterization of NGF Nanofibrous Gradient Scaffolds. To determine the secondary structure of electrospun fibers and the potential influence of the incorporated molecules, FTIR was used and structure was correlated to absorption peaks for silk. Peak assignments were as described in literature[31,35] with absorption bands in the frequency range of 1610−1625 cm^{-1} representing β-sheet structure; 1650, 1640, and 1630 cm^{-1} for coiled-coil fingerprints, and peaks above 1660 cm^{-1} ascribed to β-turns (Figure 4). There was no significant difference in the secondary structure between the treatment conditions for the mats, as electrospun fibers displayed 52−56% β sheet content, 20−30% turn structures, and 15−23% random coil/α helix structures (Figure 4D). Thus, the additives did not alter secondary structure of the silk figures.

Electrospinning allowed silk fibers to be obtained with an average diameter of 672 ± 82 nm. The oscillating ground

system controlled fiber orientation with 99,99% at an angle of deviation less than 5° and 85% less than 2°. This electrospinning approach provided regular fiber diameter with good alignment (Figure 3). No changes in average diameter or in alignment were observed between the silk fibers, the functionalized silk fibers or the gradient silk systems. The fiber density along the gradient was also measured for the four different areas. Area 0 (without NGF), 144.1 ± 21.1 fibers/mm^2; Area 5 pg/mL, 378.3 ± 43.6 fibers/mm^2; Area 50 pg/mL, 572.5 ± 46.2 fibers/mm^2; Area 500 pg/mL, 832.5 ± 75.7 fibers/mm^2. Moreover, the surface roughness of the silk fibers was about 1 nm[36] with no significant difference along the fibers and between functionalized and nonfunctionalized fibers.

3.4. NGF Functionalization and Release from Electrospun Fibers. NGF release from the electrospun silk fibers was not detected over 5 days (Figure 5A). Suggesting that the growth factors were strongly adsorbed to the nanofibers. To confirm this supposition, the functionalized fibers were dissolved in lithium bromide and after 5 days of soaking in PBS residual NGF was determined by ELISA (Figure 5A). A total of 27.5 pg/mL of NGF was detected from this dissolution process, to confirm that the NGF was still present in the fibers.

The stability of NFG was observed in a PBS − Tween20 containing 120 pg/mL of NGF during 5 days. The initial concentration was stable for the first 3 days and after 5 days 12.5% of the NGF was detected by ELISA in the solution (Figure 5B). These results suggest a protein degradation happening only after the initial 3 days that could not explain why NGF remained undetectable in our release experiments (Figure 5A).

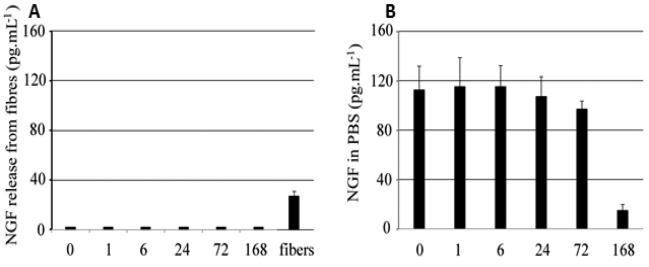

Figure 5. NGF release from electrospun functionalized silk. (A) No NGF release was detected from the silk electrospun after 5 days in PBS with 0.02% Tween20, whereas 27,5 pg mL^{-1} of NGF was detected in the electrospun mat dissolved by LiBr after 5 days. (B) Degradation of NGF was observed in PBS with 0.02% Tween20. After 3 days, more than 80% of NGF could be detected and 15% after 5 days.

These results show that the NGF was stably entrapped into the electrospun silk fibers and protected from degradation over 5 days, thus the silk fibers can be functionalized as an NGF sink to control neuronal outgrowth at the surface over extended time frames.

3.5. Neuron Growth Rate and Orientation on Constant and Gradient Concentrations of NGF-Functionalized Fibers. We have shown previously that functionalized aligned silk nanofibers allowed adhesion and guided neurons for peripheral nerve regeneration.[36] In the case of a peripheral nerve trauma, axonal outgrowth is essential for completely recovery; Therefore, a gradient of growth factors could improve alignment of axonal outgrowth, stimulate this outgrowth and also manage directionality. Primary sensory neuron cells were used to study gradient impact on nerve guidance. After 48 h of culture, the effect of silk loaded with NGF at constant concentrations (5, 50, and 500 ng/mL, respectively) was compared to silk fibers with the concentration gradient of NGF (5, 50, 500 ng/mL). For the constant concentration of NGF, lower concentrations of NGF showed that axons were not well aligned and axonal length was minimal (Figure 6A, B). In contrast, for high concentrations of NGF neurons displayed long neurite extensions and were aligned in the two directions provided by the fibers (Figure 6C).

In the gradient conditions, the axons aligned even at the low concentrations, unlike the uniform concentrations conditions (Figure 6D, E). High concentrations of NGF, 500 ng/mL, allowed better axonal outgrowth than single concentrations, and this outgrowth was orientated in one direction (Figure 6F).

Moreover, the neurons cultured with a single concentrations of NGF presented many neurite extensions while neurons cultured in the gradient conditions displayed only two neurites per cell (one smaller than the other). At high concentrations of NGF, neurite extensions in the gradient conditions were longer than those found using uniform concentrations and these

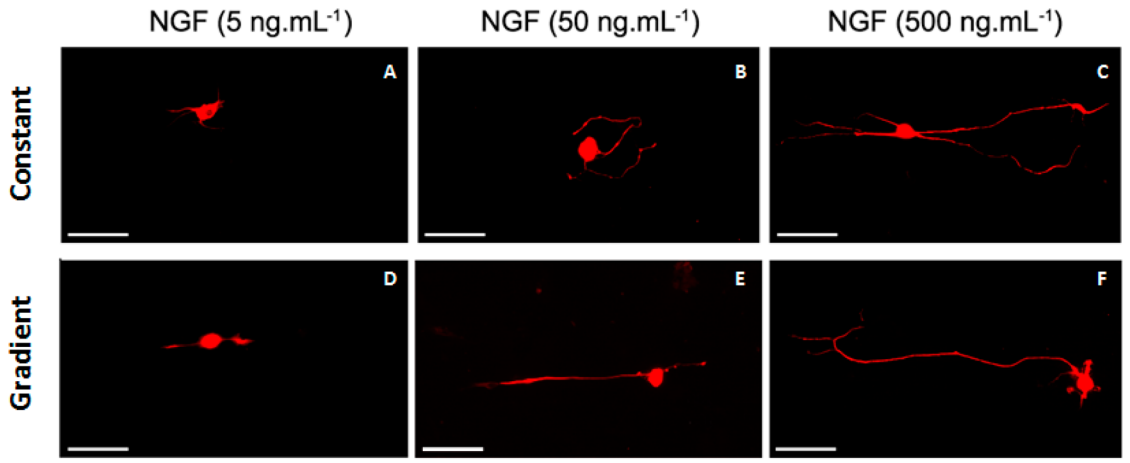

Figure 6. Neuron morphology on NGF silk electrospun and NGF gradient silk electrospun fibers. Neurons from DRGs were seeded on NGF-functionalized electrospun fibers at constant 5, 50, and 500 ng/mL^{-1} (A, B, and C, respectively), or NGF-functionalized gradient electrospun at same concentration 5, 50, and 500 ng/mL^{-1} (D, E, and F, respectively). Fluorescence images were acquired after 2 days of culture and neurons were stained with antiBIII tubulin antibody. For details see Material and Methods. Scale bars: 50 μm.

features promoted axonal outgrowth in the same direction as the gradient concentration.

3.6. Quantitative Assessment of the Axonal Outgrowth in Constant versus Gradient Conditions of NGF Concentration. To evaluate axonal outgrowth depending on the gradient, two parameters were assessed to identify biological effects of the functionalized dual gradient silk, the average length of the longest neurite and the number of neurites per cell. The longest neurite from the primary dendrite of the DRG neurons were measured on the silk fibers, silk fibers functionalized with the single concentration of NGF or the NGF gradients (Figure 7A). For the electrospun silk fibers

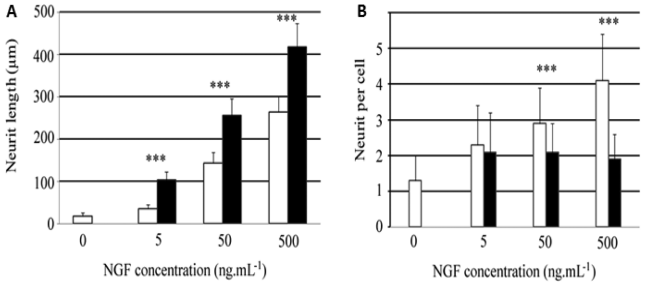

Figure 7. NGF gradient bioactivity comparing NGF constant concentration on neuron cells from DRGs. (A) Average neurite length after 2 days of culture on control fibroin nanofibers, 5, 50, 500 ng/mL of NGF in single concentration conditions (white) against 5, 50, and 500 ng/mL of NGF in gradient conditions (black). (B) Average number of neurites per cell, after 2 days of culture on control fibroin nanofibers, single concentration (white) and gradient concentration (black) of NGF; For neurite length, at least 100 neurons have been analyzed per condition measuring the longest neurite extension from neurons. (***, $p < 0{,}001$).

without NGF used as control, few surviving cells were able to extend neurites, with an average length of 17.7 ± 8.4 μm, suggesting that silk fibers supportted nerve growth. Loading NGF (at different concentrations) with silk fibers led to a significant increase in neurite length between the single and gradient conditions. At 5 ng/mL, the average of the longest neurite extension measured was 34.9 ± 10.7 μm in the mats with uniform concentration compared to 103.3 ± 19.7 μm in the gradient conditions; a 3-fold increase depending on the conditions. At 50 ng/mL, the difference between uniform and gradient conditions decreased to 1.8-fold but was still statistically significant. The average neurite length was 143.0 ± 25.3 μm in the single concentration conditions compared to 255.9 ± 40.4 μm in the gradient conditions. Finally, at 500 ng/mL, the single concentration showed an average neurite length at 264.5 ± 37.6 μm whereas on the gradients, 417.6 ± 55.7 μm was measured, a 1.6-fold difference.

For the number of neurites per cell, the silk fibers showed an average of 1 extension, increasing to 2, 3, and 4 when the constant concentration of NGF was increased (5, 50, 500 ng/mL, respectively) (Figure 7B). Interestingly, for all gradient concentration conditions, the same value of neurite extensions per cell was found to be 2, with the standard deviation decreased when the steepness of the gradient was increased.

These results show that gradients of NGF in the fibers significantly improved neurite extensions when compared to constant concentrations of the same growth factor. The results also suggest that the number of neurites per cell was stable at 2 in the gradient conditions and the neuron cell morphology became more homogeneous by increasing the steepness of the gradient.

4. DISCUSSION

Incorporating bioactive molecules to form gradients is an important element in the design of bioactive scaffolds for tissue engineering.[37] Several strategies have already been developed to mimic the design of functionalized biomaterial scaffolds using chemical techniques in hydrogel microstructures,[38] multichannels,[39] film conduits,[24] microspheres,[40] and nanofibrous structures.[10] The present work describes the production of a dual-graduated electrospun fiber biomaterial scaffold without any post spinning treatment requirements. This technique allows a dual outcome, a concentration gradient of bioactive molecule and density fibers into a nanofibrous scaffold along the *y*-axis of nanofibers.

4.1. Fibers Diameter and Alignment. Using aligned electrospun fibrous scaffolds provide cues for cell culture and also mimics the structure and function of the extracellular matrix.[41] Some specific cells, such as peripheral nerves used as a model in this work, require a complex and precise architecture,[42] and axons, glia, and perineurium are aligned parallel to each other. Nerve regeneration is based on the recapitulation of this precise nerve tissue structure. Electrospinning provides nanofiber alignment and regular diameters that can be controlled.[43,44] Qu et al.[45] showed that electrospun silk nanofiber scaffolds supported the growth, development and migration of cultured neural cells. In order to provide the growing axons with the proper surface, we have adapted the electrospinning technique in order to fit biological requirements. An increase in cell-spreading was observed on small diameters, 400 and 800 nm, but not on larger diameters, 1200 nm, silk fiber scaffolds.[45] The process used to form aligned nanofibers conferred an average diameter to the electrospun nanofibers of 672 nm, suitable for neuron adherence and growth. This was confirmed by the dissociated DRG cells growth assays in which the fibers alone promoted slight neurite extensions. Electrospun aligned fibers provided topographical cues to direct and enhance neurite outgrowth when compared to random fibers.[46] In the literature, unidirectional contours of aligned fibers provided physical guidance to the cells,[47] facilitating axon path finding and accelerating nerve tissue regeneration.[48]

4.2. Gradient Production. Fiber alignment directs cell orientation. Creating a gradient along these aligned fibers increased the direction of cell motility.[49] Bioactive molecules were added to the electrospinning solution to form the gradient. Fluorochromes with small (479 Da) and larger (70 kDa) molecular weight were successfully incorporated directly on the spinning solution. Both of the fluorochromes were found in the electrospun fibers suggesting that a range of proteins can be added to the spinning solution. A large family of growth factors and guidance cues[50] or ECM proteins[51] could be added to the spinning solution and used to develop other types of gradients. With this technique, two different molecules can be added to the solution at increasing and/or decreasing concentrations in order to control complex biological interactions. It is also possible to change molecules at each step of the electrospinning process, thus not forming a gradient but alternating areas between molecules in a scaffold for regional biofunctionalization.

4.3. NGF Functionalization. NGF interactions with silk fibers relies mainly on ionic interactions.[52] No changes to silk

secondary structure occurred as expected. Based on previous experience with growth factor incorporation and release from electrospun silk scaffolds[16,32] we did not expect NGF incorporation to affect overall β sheet content, as confirmed by the FTIR data after water annealing to promote β sheet content in the present work. Moreover, at neutral pH, silk fibroin is negatively charged (pI = 4.3) and NGF (pI = 9.3) is positively charged.[52] The molecular weight of NGF (27 kDa) may also impede diffusion. These biophysical factors of charge and size can explain the lack of release observed in the experiments by ELISA. Interestingly, fiber-entrapped NGF was protected from degradation while preserving biological activity, as evidenced by the primary neuron growth.

4.4. Neurite Extension. Neural cells are often cultured with neurobasal and constant concentration of nerve specific growth factors as brain-derived neurotrophic factor, ciliary neurotrophic factor, neurotrophin-3, NGF to promote axonal outgrowth.[53,54] To date, gradients of NGF in 3D micropatterned neural cultures have been performed to influence the formation of synapses.[55] Nerve cell migration is dependent on the chemical, mechanical and electrical properties of the substrates. The present work showed that neurite outgrowth was improved on NGF concentration gradients than with a constant concentration of NGF. Moreover, by using a four step gradient of the NGF, neurite extension was 209 μm/day compared to 132 μm/day in the constant concentration. These results demonstrate that biological activity was increased by the gradients. These gradient mats were able to stimulate increased peripheral nerve regeneration compared to those formed with a single concentration. Many efforts have been pursued for the design of complex architectures and scaffold structures to guide nerve regeneration. The introduction of these directional cues has the potential to improve the outcome for peripheral nerve repair. NGF gradients can also act as not only chemical directional cues but also a driving force for neurite outgrowth.[24]

This technique can be generally extended into different scaffolds to immobilize more than one bioactive molecule for other types of tissues as well. For example, the possibility of coupling two bioactive molecules in the scaffold gradients could be a strategy to generate new scaffolds for tendon grafts. The largest challenge in tendon grafts is the difficulty of merging two interconnected tissue types such as muscle−tendon or tendon−bone junctions.[25,56,57] This is important for both cell orientation and for the reliable mechanical properties necessary for controlled muscle, tendon, or ligament functions. Such mechanical characteristics may be achieved by modulating silk nanofiber density.

5. CONCLUSIONS

A dual-gradient aligned, NGF-loaded, silk electrospun nanofiber system was developed and characterized. To the best of our knowledge, this is the first demonstration of a double gradient with bioactive molecules and silk nanofibers density without the need for any post spinning treatments. Loading NGF in silk fibers showed that the secondary structure of the silk-fibers was not altered. This new aligned electrospun nanofiber-based materiel displayed a discontinuous concentration of NGF, which was not released from silk electrospun fibers. The impact of the concentration gradient was highlighted by the increase in neuron growth rate compared to the single concentration NGF functionalization. This gradient configuration also induced unidirectional growth of neurons, which may be of interest for applications such as nerve reconstruction. This versatile electrospining-gradient method may be used to develop other kinds of electrospun matrices for broader applications in tissue engineering and regenerative medicine.

AUTHOR INFORMATION

Corresponding Author

*E-mail: tony.dinis@utc.fr. Tel: + 33 3 44 23 44 23.

Author Contributions

The manuscript was written through contributions of all authors. All authors have given approval to the final version of the manuscript.

Notes

The authors declare no competing financial interest.

ACKNOWLEDGMENTS

This work was supported by a grant of the region Picardie through the Silknerve project, the Tissue Engineering Resource Center (TERC, P41 EB002520) from Tufts University. We also thank Raphael Turcotte for his help on SEM analysis and for contributing to morphologic measurements of fibers. Tony M. Dinis received a fellowship from the French Ministry of Science and Technology.

REFERENCES

(1) Ichihara, S.; Inada, Y.; Nakamura, T. Artificial Nerve Tubes and Their Application for Repair of Peripheral Nerve Injury: An Update of Current Concepts. *Injury* **2008**, *39* (Suppl 4), 29−39.

(2) Horner, P. J.; Gage, F. H. Regenerating the Damaged Central Nervous System. *Nature* **2000**, *407*, 963−970.

(3) Dellon, A. L.; Mackinnon, S. E. An Alternative to the Classical Nerve Graft for the Management of the Short Nerve Gap. *Plast. Reconstr. Surg.* **1988**, *82*, 849−856.

(4) Liao, C.-D.; Zhang, F.; Guo, R.-M.; Zhong, X.-M.; Zhu, J.; Wen, X.-H.; Shen, J. Peripheral Nerve Repair: Monitoring by Using Gadofluorine M-Enhanced MR Imaging with Chitosan Nerve Conduits with Cultured Mesenchymal Stem Cells in Rat Model of Neurotmesis. *Radiology* **2012**, *262*, 161−171.

(5) Biazar, E.; Khorasani, M. T.; Zaeifi, D. Nanotechnology for Peripheral Nerve Regeneration. *Int. J. Nano Dimens.* **2010**, *1*, 1−23.

(6) Hsu, S.-H.; Chan, S.-H.; Weng, C.-T.; Yang, S.-H.; Jiang, C.-F. Long-Term Regeneration and Functional Recovery of a 15 Mm Critical Nerve Gap Bridged by Tremella Fuciformis Polysaccharide-Immobilized Polylactide Conduits. *J. Evidence-Based Complementary Altern. Med.* **2013**, *2013*, 959261.

(7) Masaeli, E.; Morshed, M.; Nasr-Esfahani, M. H.; Sadri, S.; Hilderink, J.; van Apeldoorn, A.; van Blitterswijk, C. A.; Moroni, L. Fabrication, Characterization and Cellular Compatibility of Poly-(hydroxy Alkanoate) Composite Nanofibrous Scaffolds for Nerve Tissue Engineering. *PLoS One* **2013**, *8*, e57157.

(8) Liu, T.; Houle, J. D.; Xu, J.; Chan, B. P.; Chew, S. Y. Nanofibrous Collagen Nerve Conduits for Spinal Cord Repair. *Tissue Eng., Part A* **2012**, *18*, 1057−1066.

(9) Kehoe, S.; Zhang, X. F.; Boyd, D. FDA Approved Guidance Conduits and Wraps for Peripheral Nerve Injury: A Review of Materials and Efficacy. *Injury* **2012**, *43*, 553−572.

(10) Zhang, X.; Baughman, C. B.; Kaplan, D. L. In Vitro Evaluation of Electrospun Silk Fibroin Scaffolds for Vascular Cell Growth. *Biomaterials* **2008**, *29*, 2217−2227.

(11) Zhang, X.; Reagan, M. R.; Kaplan, D. L. Electrospun Silk Biomaterial Scaffolds for Regenerative Medicine. *Adv. Drug Delivery Rev.* **2009**, *61*, 988−1006.

(12) Altman, G. H.; Diaz, F.; Jakuba, C.; Calabro, T.; Horan, R. L.; Chen, J.; Lu, H.; Richmond, J.; Kaplan, D. L. Silk-Based Biomaterials. *Biomaterials* **2003**, *24*, 401−416.

(13) Meinel, L.; Hofmann, S.; Karageorgiou, V.; Kirker-Head, C.; McCool, J.; Gronowicz, G.; Zichner, L.; Langer, R.; Vunjak-Novakovic, G.; Kaplan, D. L. The Inflammatory Responses to Silk Films in Vitro and in Vivo. *Biomaterials* **2005**, *26*, 147−155.
(14) Cohen-Karni, T.; Jeong, K. J.; Tsui, J. H.; Reznor, G.; Mustata, M.; Wanunu, M.; Graham, A.; Marks, C.; Bell, D. C.; Langer, R.; Kohane, D. S. Nanocomposite Gold-Silk Nanofibers. *Nano Lett.* **2012**, *12*, 5403−5406.
(15) Sofroniew, M. V.; Howe, C. L.; Mobley, W. C. Nerve Growth Factor Signaling, Neuroprotection, and Neural Repair. *Annu. Rev. Neurosci.* **2001**, *24*, 1217−1281.
(16) Li, C.; Vepari, C.; Jin, H.-J.; Kim, H. J.; Kaplan, D. L. Electrospun Silk-BMP-2 Scaffolds for Bone Tissue Engineering. *Biomaterials* **2006**, *27*, 3115−3124.
(17) Schneider, A.; Wang, X. Y.; Kaplan, D. L.; Garlick, J. A.; Egles, C. Biofunctionalized Electrospun Silk Mats as a Topical Bioactive Dressing for Accelerated Wound Healing. *Acta Biomater.* **2009**, *5*, 2570−2578.
(18) Sahoo, S.; Ang, L. T.; Goh, J. C.-H.; Toh, S.-L. Growth Factor Delivery through Electrospun Nanofibers in Scaffolds for Tissue Engineering Applications. *J. Biomed. Mater. Res., Part A* **2010**, *93A*, 1539−1550.
(19) Varkey, M.; Gittens, S. A.; Uludag, H. Growth Factor Delivery for Bone Tissue Repair: An Update. *Expert Opin. Drug Delivery* **2004**, *1*, 19−36.
(20) Campenot, R. B. Local Control of Neurite Development by Nerve Growth Factor. *Proc. Natl. Acad. Sci. U.S.A.* **1977**, *74*, 4516−4519.
(21) Tessier-Lavigne, M.; Goodman, C. S. The Molecular Biology of Axon Guidance. *Science* **1996**, *274*, 1123−1133.
(22) Kang, C. E.; Gemeinhart, E. J.; Gemeinhart, R. A. Cellular Alignment by Grafted Adhesion Peptide Surface Density Gradients. *J. Biomed. Mater. Res., Part A* **2004**, *71*, 403−411.
(23) Shi, J.; Wang, L.; Zhang, F.; Li, H.; Lei, L.; Liu, L.; Chen, Y. Incorporating Protein Gradient into Electrospun Nanofibers as Scaffolds for Tissue Engineering. *ACS Appl. Mater. Interfaces* **2010**, *2*, 1025−1030.
(24) Tang, S.; Zhu, J.; Xu, Y.; Xiang, A. P.; Jiang, M. H.; Quan, D. The Effects of Gradients of Nerve Growth Factor Immobilized PCLA Scaffolds on Neurite Outgrowth in Vitro and Peripheral Nerve Regeneration in Rats. *Biomaterials* **2013**, *34*, 7086−7096.
(25) Samavedi, S.; Guelcher, S. A.; Goldstein, A. S.; Whittington, A. R. Response of Bone Marrow Stromal Cells to Graded Co-Electrospun Scaffolds and Its Implications for Engineering the Ligament-Bone Interface. *Biomaterials* **2012**, *33*, 7727−7735.
(26) Mai, J.; Fok, L.; Gao, H.; Zhang, X.; Poo, M.-M. Axon Initiation and Growth Cone Turning on Bound Protein Gradients. *J. Neurosci.* **2009**, *29*, 7450−7458.
(27) Thompson, A. W.; Pujic, Z.; Richards, L. J.; Goodhill, G. J. Cyclic Nucleotide-Dependent Switching of Mammalian Axon Guidance Depends on Gradient Steepness. *Mol. Cell. Neurosci.* **2011**, *47*, 45−52.
(28) Leslie-Barbick, J. E.; Shen, C.; Chen, C.; West, J. L. Micron-Scale Spatially Patterned, Covalently Immobilized Vascular Endothelial Growth Factor on Hydrogels Accelerates Endothelial Tubulogenesis and Increases Cellular Angiogenic Responses. *Tissue Eng., Part A* **2011**, *17*, 221−229.
(29) Kothapalli, C. R.; van Veen, E.; de Valence, S.; Chung, S.; Zervantonakis, I. K.; Gertler, F. B.; Kamm, R. D. A High-Throughput Microfluidic Assay to Study Neurite Response to Growth Factor Gradients. *Lab Chip* **2011**, *11*, 497−507.
(30) Rockwood, D. N.; Preda, R. C.; Yücel, T.; Wang, X.; Lovett, M. L.; Kaplan, D. L. Materials Fabrication from Bombyx Mori Silk Fibroin. *Nat. Protoc.* **2011**, *6*, 1612−1631.
(31) Jin, H.-J.; Park, J.; Karageorgiou, V.; Kim, U.-J.; Valluzzi, R.; Cebe, P.; Kaplan, D. L. Water-Stable Silk Films with Reduced B-Sheet Content. *Adv. Funct. Mater.* **2005**, *15*, 1241−1247.
(32) Hu, X.; Shmelev, K.; Sun, L.; Gil, E.-S.; Park, S.-H.; Cebe, P.; Kaplan, D. L. Regulation of Silk Material Structure by Temperature-Controlled Water Vapor Annealing. *Biomacromolecules* **2011**, *12*, 1686−1696.
(33) Malin, S. A.; Davis, B. M.; Molliver, D. C. Production of Dissociated Sensory Neuron Cultures and Considerations for Their Use in Studying Neuronal Function and Plasticity. *Nat. Protoc.* **2007**, *2*, 152−160.
(34) Jin, H.-J.; Chen, J.; Karageorgiou, V.; Altman, G. H.; Kaplan, D. L. Human Bone Marrow Stromal Cell Responses on Electrospun Silk Fibroin Mats. *Biomaterials* **2004**, *25*, 1039−1047.
(35) Zhu, M.; Wang, K.; Mei, J.; Li, C.; Zhang, J.; Zheng, W.; An, D.; Xiao, N.; Zhao, Q.; Kong, D.; Wang, L. Fabrication of Highly Interconnected Porous Silk Fibroin Scaffolds for Potential Use as Vascular Grafts. *Acta Biomater.* **2014**, *10*, 2014−2023.
(36) Wittmer, C. R.; Claudepierre, T.; Reber, M.; Wiedemann, P.; Garlick, J. A.; Kaplan, D.; Egles, C. Multifunctionalized Electrospun Silk Fibers Promote Axon Regeneration in Central Nervous System. *Adv. Funct. Mater.* **2011**, *21*, 4202.
(37) Roam, J. L.; Xu, H.; Nguyen, P. K.; Elbert, D. L. The Formation of Protein Concentration Gradients Mediated by Density Differences of Poly(ethylene Glycol) Microspheres. *Biomaterials* **2010**, *31*, 8642−8650.
(38) Richardson, S. M.; Curran, J. M.; Chen, R.; Vaughan-Thomas, A.; Hunt, J. A.; Freemont, A. J.; Hoyland, J. A. The Differentiation of Bone Marrow Mesenchymal Stem Cells into Chondrocyte-like Cells on Poly-L-Lactic Acid (PLLA) Scaffolds. *Biomaterials* **2006**, *27*, 4069−4078.
(39) Lee, K. H.; Lee, K. H.; Lee, J.; Choi, H.; Lee, D.; Park, Y.; Lee, S.-H. Integration of Microfluidic Chip with Biomimetic Hydrogel for 3D Controlling and Monitoring of Cell Alignment and Migration. *J. Biomed. Mater. Res., Part A* **2014**, *102*, 1164−1172.
(40) Roam, J. L.; Xu, H.; Nguyen, P. K.; Elbert, D. L. The Formation of Protein Concentration Gradients Mediated by Density Differences of Poly(ethylene Glycol) Microspheres. *Biomaterials* **2010**, *31*, 8642−8650.
(41) Simpson, D. G.; Terracio, L.; Terracio, M.; Price, R. L.; Turner, D. C.; Borg, T. K. Modulation of Cardiac Myocyte Phenotype in Vitro by the Composition and Orientation of the Extracellular Matrix. *J. Cell. Physiol.* **1994**, *161*, 89−105.
(42) Biazar, E.; Khorasani, M.; Montazeri, N.; Pourshamsian, K.; Daliri, M.; T, M. R.; B, M. J.; Khoshzaban, A.; K, S. H.; Jafarpour, M.; Roviemiab, Z. Types of Neural Guides and Using Nanotechnology for Peripheral Nerve Reconstruction. *Int. J. Nanomed.* **2010**, *5*, 839−852.
(43) Jose, R. R.; Elia, R.; Firpo, M. A.; Kaplan, D. L.; Peattie, R. A. Seamless, Axially Aligned, Fiber Tubes, Meshes, Microbundles and Gradient Biomaterial Constructs. *J. Mater. Sci.: Mater. Med.* **2012**, *23*, 2679−2695.
(44) Grey, C. P.; Newton, S. T.; Bowlin, G. L.; Haas, T. W.; Simpson, D. G. Gradient Fiber Electrospinning of Layered Scaffolds Using Controlled Transitions in Fiber Diameter. *Biomaterials* **2013**, *34*, 4993−5006.
(45) Qu, J.; Wang, D.; Wang, H.; Dong, Y.; Zhang, F.; Zuo, B.; Zhang, H. Electrospun Silk Fibroin Nanofibers in Different Diameters Support Neurite Outgrowth and Promote Astrocyte Migration. *J. Biomed. Mater. Res., Part A* **2013**, *101*, 2667−2678.
(46) Corey, J. M.; Lin, D. Y.; Mycek, K. B.; Chen, Q.; Samuel, S.; Feldman, E. L.; Martin, D. C. Aligned Electrospun Nanofibers Specify the Direction of Dorsal Root Ganglia Neurite Growth. *J. Biomed. Mater. Res., Part A* **2007**, *83*, 636−645.
(47) Lee, J.-H.; Lee, Y. J.; Cho, H.-J.; Shin, H. Guidance of In Vitro Migration of Human Mesenchymal Stem Cells and In Vivo Guided Bone Regeneration Using Aligned Electrospun Fibers. *Tissue Eng., Part A* **2013**, *20*, 2031−2042.
(48) Liu, X.; Chen, J.; Gilmore, K. J.; Higgins, M. J.; Liu, Y.; Wallace, G. G. Guidance of Neurite Outgrowth on Aligned Electrospun Polypyrrole/poly(styrene-Beta-Isobutylene-Beta-Styrene) Fiber Platforms. *J. Biomed. Mater. Res., Part A* **2010**, *94*, 1004−1011.
(49) Sundararaghavan, H. G.; Saunders, R. L.; Hammer, D. A.; Burdick, J. A. Fiber Alignment Directs Cell Motility over Chemotactic Gradients. *Biotechnol. Bioeng.* **2013**, *110*, 1249−1254.

(50) Vadivel, A.; Alphonse, R. S.; Collins, J. J. P.; van Haaften, T.; O'Reilly, M.; Eaton, F.; Thébaud, B. The Axonal Guidance Cue Semaphorin 3C Contributes to Alveolar Growth and Repair. *PLoS One* **2013**, *8*, e67225.
(51) Valmikinathan, C. M.; Wang, J.; Smiriglio, S.; Golwala, N. G.; Yu, X. Magnetically Induced Protein Gradients on Electrospun Nanofibers. *Comb. Chem. High Throughput Screening* **2009**, *12*, 656–663.
(52) Uebersax, L.; Mattotti, M.; Papaloïzos, M.; Merkle, H. P.; Gander, B.; Meinel, L. Silk Fibroin Matrices for the Controlled Release of Nerve Growth Factor (NGF). *Biomaterials* **2007**, *28*, 4449–4460.
(53) Sandrock, A. W., Jr.; Matthew, W. D. Substrate-Bound Nerve Growth Factor Promotes Neurite Growth in Peripheral Nerve. *Brain Res.* **1987**, *425*, 360–363.
(54) Kamei, N.; Tanaka, N.; Oishi, Y.; Hamasaki, T.; Nakanishi, K.; Sakai, N.; Ochi, M. BDNF, NT-3, and NGF Released from Transplanted Neural Progenitor Cells Promote Corticospinal Axon Growth in Organotypic Cocultures. *Spine (Philadelphia)* **2007**, *32*, 1272–1278.
(55) Kunze, A.; Valero, A.; Zosso, D.; Renaud, P. Synergistic NGF/B27 Gradients Position Synapses Heterogeneously in 3D Micropatterned Neural Cultures. *PLoS One* **2011**, *6*, e26187.
(56) Ladd, M. R.; Lee, S. J.; Stitzel, J. D.; Atala, A.; Yoo, J. J. Co-Electrospun Dual Scaffolding System with Potential for Muscle-Tendon Junction Tissue Engineering. *Biomaterials* **2011**, *32*, 1549–1559.
(57) Xie, J.; Li, X.; Lipner, J.; Manning, C. N.; Schwartz, A. G.; Thomopoulos, S.; Xia, Y. Aligned-to-Random" Nanofiber Scaffolds for Mimicking the Structure of the Tendon-to-Bone Insertion Site. *Nanoscale* **2010**, *2*, 923–926.